Comparison of Numerical Schemes to Solve the Newton-Lorentz Equation

NORTH-WEST UNIVERSITY YUNIBESITI YA BOKONE-BOPHIRIMA NOORDWES-UNIVERSITEIT POTCHEFSTROOM CAMPUS

Jabus van den Berg[1]

[1] Centre for Space Research, North-West University, Potchefstroom, South Africa

24182869@nwu.ac.za

Abstract

To better understand the transport of solar energetic particles, a conceptual understanding of the micro-physics of charged particle propagation in electric and magnetic fields is needed. The movement of charged particles are governed by the Newton-Lorentz equation, which becomes increasingly difficult to solve analytically for complicated electric and magnetic fields. In this work, the methods of Boris (1970) and Vay (2008), as well as a forth-order Runge-Kutta scheme, are investigated for numerically solving the Newton-Lorentz equation. This work focuses on accuracy rather than computational speed, since these numerical schemes will be used to analyse the motion of particles in turbulent electric and magnetic fields. The Larmor radius, deviation between the final numerical and analytical position, as well as the execution time, are calculated and recorded for different time steps.

1 The Newton-Lorentz Equation

The motion of a particle with mass m and charge q, moving with velocity $\vec{v}$ in an electric field $\vec{E}$ and magnetic field $\vec{B}$, is governed by the Newton-Lorentz equation

$$m\frac{d(\gamma\vec{v})}{dt} = q\left(\vec{E} + \vec{v}\times\vec{B}\right), \tag{1}$$

where $\gamma = 1/\sqrt{1-(v/c)^2}$ is the Lorentz factor, with c the speed of light in vacuum (Griffiths, 1999). This can be split into two, first-order differential equations

$$\frac{d\vec{r}(t)}{dt} = \vec{v}(t) \quad\text{and}\quad m\frac{d\vec{u}(t)}{dt} = q\left[\vec{E}\left(\vec{r}(t);t\right) + \vec{v}(t)\times\vec{B}\left(\vec{r}(t);t\right)\right], \tag{2}$$

where $\vec{u}(t) = \gamma(t)\vec{v}(t)$. This is solved in Cartesian coordinates since the vector product is easily calculated and it is difficult to find a symmetry axis for a general magnetic field. The numerical methods used to solve this equations should be accurate to simulate charged particles in turbulent electric and magnetic fields, as shown in Fig. 1.

The Larmor radius of the particle's gyration is defined as

$$r_L = v_\perp/\omega_c, \tag{3}$$

where $v_\perp = v\sin[\arccos(\vec{v}\cdot\vec{B}/vB)]$ is the particle's speed perpendicular to the magnetic field and

$$\omega_c = |q|B/\gamma m \tag{4}$$

is the cyclotron frequency.

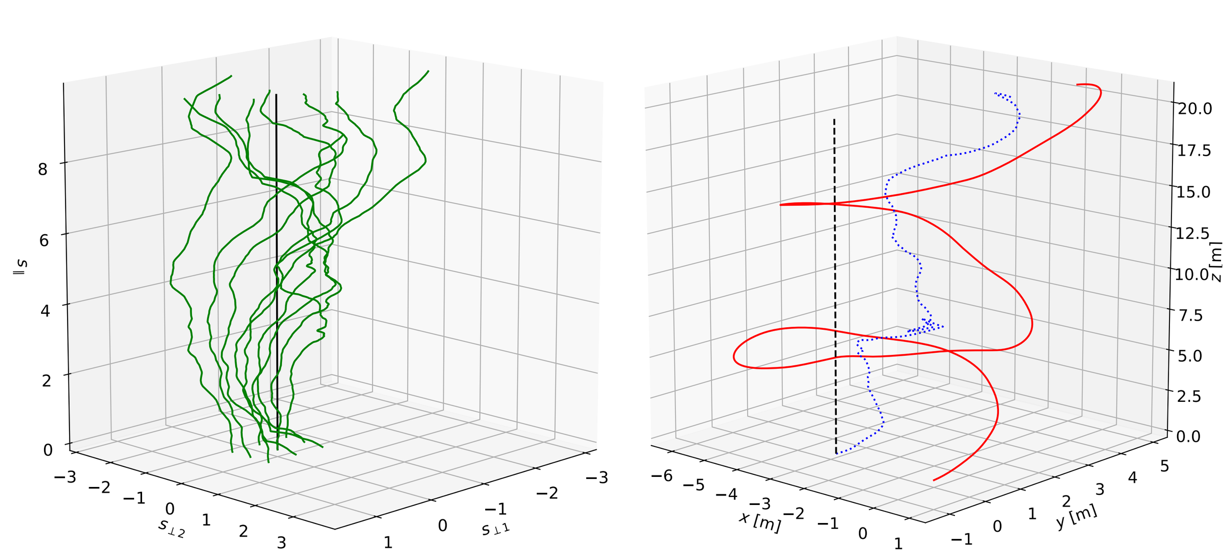

Fig. 1: *Left panel: Background (black) and turbulent (green) magnetic field lines of a composite slab-2D turbulence model at time $t=0$. The magnetic field lines can be though of as the path of the particle's guiding centre if the particle is stuck to the field line. Right panel: Trajectory (red) of an electron in the composite turbulence model, simulated using the Runge-Kutta method. A single background magnetic field line (black dashed) and the particle's guiding centre (blue dotted) is also shown.*

2.1 The Method of Boris (1970)

The position can be calculated by a time-centred approximation of Eq. 2a

$$\frac{\vec{r}_{n+1/2}-\vec{r}_{n-1/2}}{\Delta t} \approx \vec{v}_n \quad\Longrightarrow\quad \vec{r}_{n+1/2} = \vec{r}_{n-1/2} + \vec{v}_n\Delta t, \tag{5}$$

where a subscript n denotes that quantity at time $t_n = t_0 + n\Delta t$, with t_0 the initial time and $n = 0;1;2;\ldots$, and it should be remembered that $\vec{v}_n = \vec{u}_n/\gamma_n$.

Boris (1970) suggested a decoupling of the electric and magnetic field to solve Eq. 2b by first applying half of the electric field, then applying the rotation of the velocity vector by the magnetic field and lastly applying the other half of the electric field:

$$\vec{u}_- = \vec{u}_{n-1} + \frac{q\Delta t}{2m}\vec{E}_{n-1/2} \qquad \vec{u}_{n+1/2} = \vec{u}_- + f_1\vec{u}_-\times\vec{B}_{n-1/2} \tag{6a}$$

$$\vec{u}_+ = \vec{u}_- + f_2\vec{u}_{n+1/2}\times\vec{B}_{n-1/2} \qquad \vec{u}_{n+1} = \vec{u}_+ + \frac{q\Delta t}{2m}\vec{E}_{n-1/2}, \tag{6b}$$

where

$$f_1 = \tan\left(qB_{n-1/2}\Delta t/2m\gamma_-\right)/B_{n-1/2}, \tag{7a}$$

$$f_2 = 2f_1/\left[1+(f_1B_{n-1/2})^2\right] \quad\text{and}\quad \gamma_n = \sqrt{1+(u_n/c)^2}, \tag{7b}$$

with $\vec{E}_{n-1/2} = \vec{E}(\vec{r}_{n-1/2};t_{n-1/2})$, $\vec{B}_{n-1/2} = \vec{B}(\vec{r}_{n-1/2};t_{n-1/2})$ and $B_{n-1/2} = |\vec{B}_{n-1/2}|$.

2.1.1 An Approximation

Since $\tan\theta \approx \theta$ to first order in θ if $|\theta| \ll 1$, as should hold for a small time step, Eqs. 6a to 7b can be simplified (Birdsall & Langdon, 1991):

$$\vec{u}_- = \vec{u}_{n-1} + \frac{q\Delta t}{2m}\vec{E}_{n-1/2} \qquad \vec{u}_{n+1/2} = \vec{u}_+ + \vec{u}_-\times\vec{f}_1 \tag{8a}$$

$$\vec{u}_+ = \vec{u}_- + \vec{u}_{n+1/2}\times\vec{f}_2 \qquad \vec{u}_{n+1} = \vec{u}_+ + \frac{q\Delta t}{2m}\vec{E}_{n-1/2}, \tag{8b}$$

where

$$\vec{f}_1 \approx q\vec{B}_{n-1/2}\Delta t/2m\gamma_- \quad\text{and}\quad \vec{f}_2 = 2\vec{f}_1/(1+f_1^2). \tag{9}$$

2.1.2 Initial Conditions

Initially $\vec{u}_0 = \vec{v}_0/\sqrt{1-(v_0/c)^2}$ for the initial position $\vec{r}_0$ and velocity $\vec{v}_0$ at time t_0. Initially a half time step must be taken forward in the position using the initial velocity, $\vec{r}_{1/2} = \vec{r}_0 + \vec{v}_0\Delta t/2$, as Eq. 5 indicates that the position are needed at half time steps. The velocity can then be updated followed by the position. This method is illustrated in the top panel of Fig. 2.

2.2 The Method of Vay (2008)

The method of Vay (2008) does not decouple the electric and magnetic field when solving Eq. 2b, but rather applies both the electric and magnetic field during the first half time step, while applying the electric field and a rotation of the velocity vector during the second half time step:

$$\vec{u}_{n+1/2} = \vec{u}_n + \frac{q\Delta t}{2m}\left[\vec{E}_{n+1/2} + \vec{v}_n\times\vec{B}_{n+1/2}\right] \tag{10a}$$

$$\vec{u}' = \vec{u}_{n+1/2} + \frac{q\Delta t}{2m}\vec{E}_{n+1/2} \qquad \vec{u}_{n+1} = s\left[\vec{u}' + (\vec{u}'\cdot\vec{f})\vec{f} + \vec{u}'\times\vec{f}\right], \tag{10b}$$

where

$$\vec{b} = \frac{q\Delta t}{2m}\vec{B}_{n+1/2}, \qquad \vec{f} = \frac{\vec{b}}{\gamma_{n+1}}, \qquad s = \frac{1}{1+f^2} \tag{11}$$

and

$$\gamma_{n+1} = \sqrt{0.5\sigma + 0.5\sqrt{\sigma^2 + 4(b^2+u_*^2)}}, \tag{12a}$$

$$u_* = (\vec{u}'\cdot\vec{b})/c, \qquad \gamma_* = \sqrt{1+(u'/c)^2}, \qquad \sigma = \gamma_*^2 - b^2. \tag{12b}$$

2.2.1 Initial Conditions

Initially $\vec{u}_0 = \vec{v}_0/\sqrt{1-(v_0/c)^2}$ for the initial position $\vec{r}_0$ and velocity $\vec{v}_0$ at time t_0. Initially a half time step must be taken backward in the position using the initial velocity, $\vec{r}_{-1/2} = \vec{r}_0 - \vec{v}_0\Delta t/2$, as $\vec{r}_{n+1/2}$ is needed to update the velocity. The position can then be updated followed by the velocity. This method is illustrated in the bottom panel of Fig. 2.

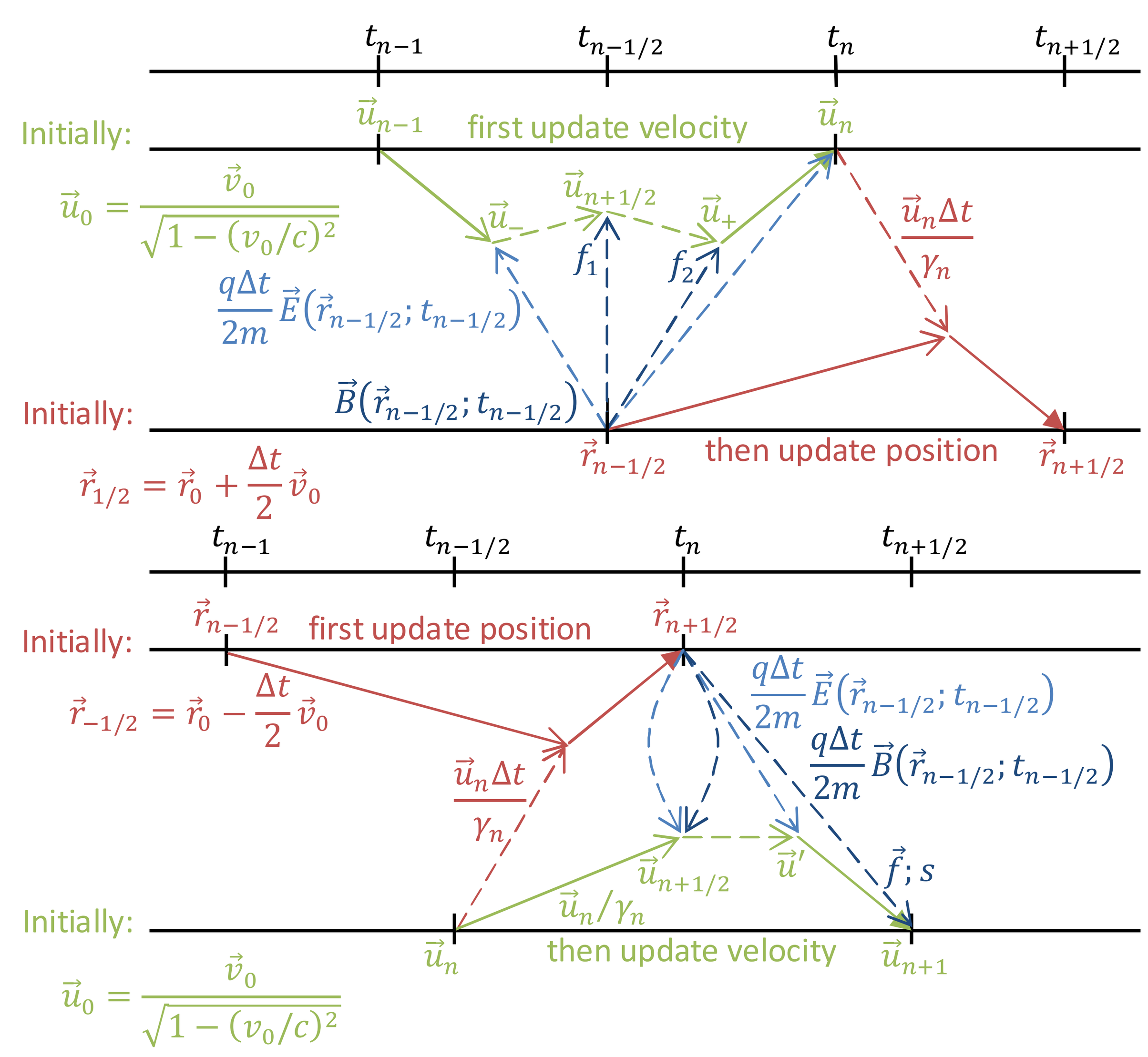

Fig. 2: Top: *Schematic representation of the method of Boris (1970).* Bottom: *Schematic representation of the method of Vay (2008).*

2.3 The Runge-Kutta Method

For the Runge-Kutta method, Eq. 2b should be rewritten in terms of the time derivative of only $\vec{v}$ and not $\vec{u}$, such that

$$\frac{d\vec{v}}{dt} = \frac{q}{\gamma m}\left[\vec{E} + \vec{v}\times\vec{B} - \frac{\vec{v}\cdot\vec{E}}{c^2}\vec{v}\right], \tag{13}$$

where the additional last term can be thought of as the rate of change of the Lorentz factor due to the electric field in terms of the velocity (Griffiths, 1999). The Runge-Kutta scheme for solving the set of differential equations

$$\frac{d\vec{X}(t)}{dt} = \vec{f}\left(t;\vec{X}(t)\right)$$

of the unknown functions $\vec{X}(t)$, are

$$\vec{X}_{n+1} = \vec{X}_n + \frac{\Delta t}{6}\left(\vec{k}_1 + 2\vec{k}_2 + 2\vec{k}_3 + \vec{k}_4\right), \tag{14}$$

where

$$\vec{k}_1 = \vec{f}\left(t_n;\vec{X}_n\right), \qquad \vec{k}_2 = \vec{f}\left(t_{n+1/2};\vec{X}_n + \vec{k}_1\Delta t/2\right) \tag{15a}$$

$$\vec{k}_3 = \vec{f}\left(t_{n+1/2};\vec{X}_n + \vec{k}_2\Delta t/2\right) \qquad \vec{k}_4 = \vec{f}\left(t_{n+1};\vec{X}_n + \vec{k}_3\Delta t\right) \tag{15b}$$

(Edwards & Penney, 2008). Here the unknown functions are $\vec{X}(t) = [x(t)\;\; y(t)\;\; z(t)\;\; v_x(t)\;\; v_y(t)\;\; v_z(t)]^T$ and the functions describing the differential equations are

$$\vec{f}\left(t;\vec{X}(t)\right) = \begin{bmatrix} v_x(t) \\ v_y(t) \\ v_z(t) \\ \frac{q}{\gamma m}\left\{E_x(\vec{r};t) + \left[\vec{v}(t)\times\vec{B}(\vec{r};t)\right]_x - \frac{\vec{v}(t)\cdot\vec{E}(\vec{r};t)}{c^2}v_x(t)\right\} \\ \frac{q}{\gamma m}\left\{E_y(\vec{r};t) + \left[\vec{v}(t)\times\vec{B}(\vec{r};t)\right]_y - \frac{\vec{v}(t)\cdot\vec{E}(\vec{r};t)}{c^2}v_y(t)\right\} \\ \frac{q}{\gamma m}\left\{E_z(\vec{r};t) + \left[\vec{v}(t)\times\vec{B}(\vec{r};t)\right]_z - \frac{\vec{v}(t)\cdot\vec{E}(\vec{r};t)}{c^2}v_z(t)\right\} \end{bmatrix}, \tag{16}$$

where the Lorentz factor γ is defined in the normal way.

3 Numerical Setup

The numerical methods are implemented in Python, making use of the NumPy package. In what follows, an electron is simulated in a zero electric field and a constant magnetic field $\vec{B} = 1\hat{z}\ \mathrm{nT}$ initialized at time $t_0 = 0\ \mathrm{s}$ with a velocity $\vec{v}_0 = (1\hat{x} + 0.1\hat{z})\ \mathrm{m\cdot s^{-1}}$ at the position $\vec{r}_0 = \vec{0}\ \mathrm{m}$. The integration are preformed for 10 gyrations ($N_t = \mathrm{int}[20\pi/\omega_c\Delta t]$) and $N_{spg} = 2^i$ steps per gyration, with $i = 0;1;\cdots;20$, that is with time steps $\Delta t = 2\pi/\omega_c N_{spg}$ s. For each of these simulations the Larmor radius, deviation between the final numerical and analytical position and execution time are calculated and recorded.

3.1 Stability

Deviations from the true Larmor radius are significant for large time steps in the Runge-Kutta method. Deviations occur at the floating point accuracy for the Boris and Vay method. Overall, the Larmor radius stays constant with time and is independent of the time step, implying that the numerical methods do not numerically change the particle's energy. See Fig. 3.

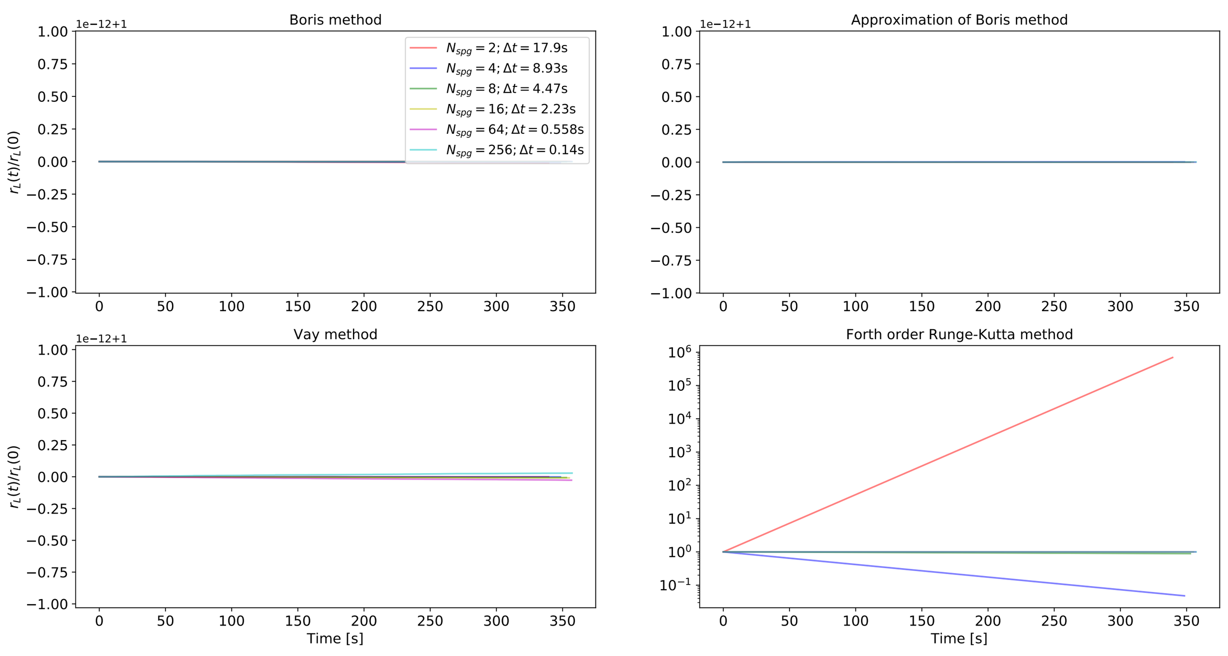

Fig. 3: *Ratio of temporal Larmor radii $r_L(t)$ to initial Larmor radius $r_L(0)$ as a function of time for different number of steps per gyration N_{spg}.*

3.2 Order of Accuracy

By fitting the function

$$\frac{\left|\vec{r}^{\,anl}_{N_t} - \vec{r}^{\,num}_{N_t}\right|}{r_L(0)} = D\left(\omega_c\Delta t\right)^O, \tag{17}$$

the order of convergence O can be calculated, where D is a constant (Schutte, 2016). The methods do not converge for large time steps and for small time steps the accuracy is limited by the floating point accuracy. The order of accuracy is indicated in the legend of Fig. 4.

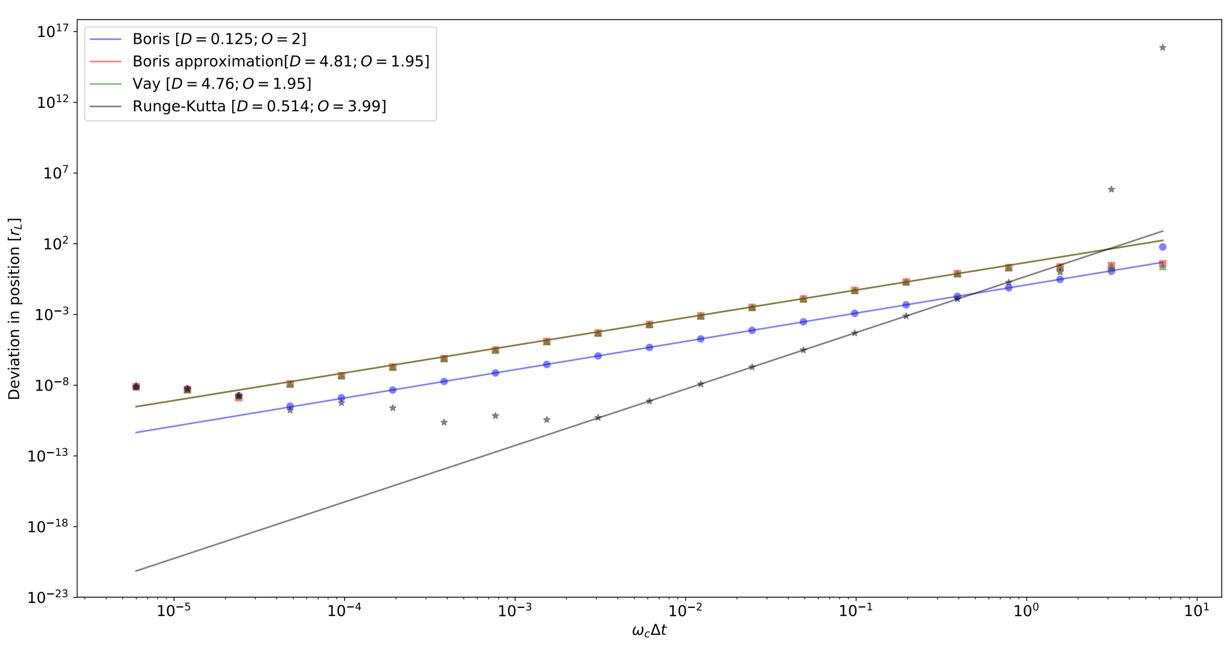

Fig. 4: *Deviation between numerical and analytical end position in units of the initial Larmor radius, as a function of the time step multiplied by the cyclotron frequency. The result of fitting Eq. 17 are indicated in the legend, giving the order of accuracy O of the numerical method.*

3.3 Execution Time

The Runge-Kutta method is slightly slower than the other two methods and the evaluation of the tangent function in the Boris method does not seem to add additional execution time, except for large time steps. See Fig. 5.

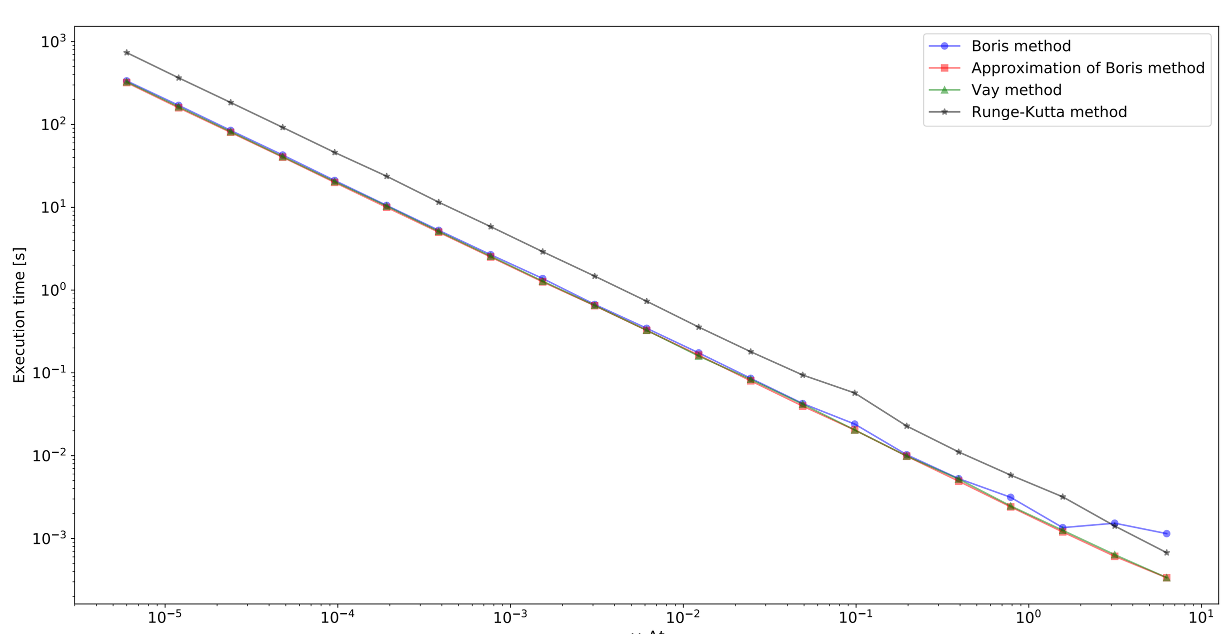

Fig. 5: *Execution time as a function of time step multiplied by the cyclotron frequency.*

4 Conclusion

The methods do not numerically change the energy of the particle, except the Runge-Kutta method for large time steps.

The methods do not converge for large time steps and the accuracy is limited by the floating point accuracy for small time steps.

The Boris and Vay methods are second-order accurate, while the Runge-Kutta method is forth-order accurate.

The Runge-Kutta method is slightly slower than the other two methods and the evaluation of the tangent function in the Boris method does not add additional execution time, except for large time steps.

A balance between accurate results and execution time suggest 16 steps per gyration for the Boris and Vay methods and 8 steps per gyration for the Runge-Kutta method.

References:

Birdsall, C.K. & Langdon, A.B. 1991. Plasma physics via computer simulation (Adam Hilger).

Boris, J.P. 1970. Relativistic plasma simulation: optimization of a hybrid code. Numerical Simulation of Plasmas Conference Proceedings, 4, 3–67.

Edwards, C.H. & Penney, D.E. 2008. Elementary differential equations with boundary value problems. Sixth ed. (Pearson Education, Edinburg Gate).

Griffiths, D.J. 1999. Introduction to electrodynamics. Third ed. (Prentice Hall, Upper Saddle River, New Jersey).

Schutte, H.M. 2016. Particle push comparisons. Hons.B.Sc. dissertation. Potchefstroom Campus of the North-West University, South Africa.

Vay, J.L. 2008. Simulation of beams or plasmas crossing at relativistic velocity. Physics of Plasmas, 15.